

FEATURES

- Low offset voltage: 65 μ V maximum**
- Low input bias currents: 1 pA maximum**
- Low noise: 8 nV/ $\sqrt{\text{Hz}}$**
- Wide bandwidth: 10 MHz**
- High open-loop gain: 1000 V/mV**
- Unity gain stable**
- Single-supply operation: 2.7 V to 5.5 V**
- 5-ball WLCSP for single (AD8605) and 8-ball WLCSP for dual (AD8606)**

APPLICATIONS

- Photodiode amplification**
- Battery-powered instrumentation**
- Multipole filters**
- Sensors**
- Barcode scanners**
- Audio**

GENERAL DESCRIPTION

The AD8605, AD8606, and AD8608¹ are single, dual, and quad rail-to-rail input and output, single-supply amplifiers. They feature very low offset voltage, low input voltage and current noise, and wide signal bandwidth. They use the Analog Devices, Inc. patented DigiTrim[®] trimming technique, which achieves superior precision without laser trimming.

The combination of low offsets, low noise, very low input bias currents, and high speed makes these amplifiers useful in a wide variety of applications. Filters, integrators, photodiode amplifiers, and high impedance sensors all benefit from the combination of performance features. Audio and other ac applications benefit from the wide bandwidth and low distortion. Applications for these amplifiers include optical control loops, portable and loop-powered instrumentation, and audio amplification for portable devices.

The AD8605, AD8606, and AD8608 are specified over the extended industrial temperature range (-40°C to $+125^{\circ}\text{C}$). The AD8605 single is available in 5-lead SOT-23 and 5-ball WLCSP packages. The AD8606 dual is available in an 8-lead MSOP, an 8-ball WLCSP, and a narrow SOIC surface-mounted package. The AD8608 quad is available in a 14-lead TSSOP package and a narrow 14-lead SOIC package. The 5-ball and 8-ball WLCSP offer the smallest available footprint for any surface-mounted operational amplifier. The WLCSP, SOT-23, MSOP, and TSSOP versions are available in tape-and-reel only.

¹ Protected by U.S. Patent No. 5,969,657.

Rev. O

Document Feedback

Information furnished by Analog Devices is believed to be accurate and reliable. However, no responsibility is assumed by Analog Devices for its use, nor for any infringements of patents or other rights of third parties that may result from its use. Specifications subject to change without notice. No license is granted by implication or otherwise under any patent or patent rights of Analog Devices. Trademarks and registered trademarks are the property of their respective owners.

PIN CONFIGURATIONS

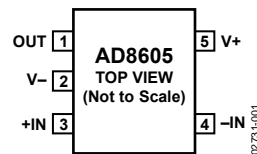


Figure 1. 5-Lead SOT-23 (RJ Suffix)

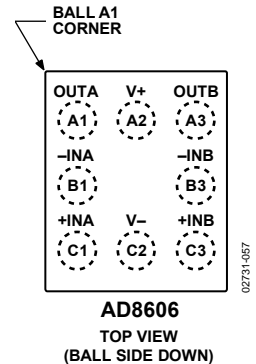


Figure 2. 8-Ball WLCSP (CB Suffix)

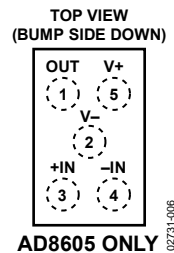


Figure 3. 5-Ball WLCSP (CB Suffix)

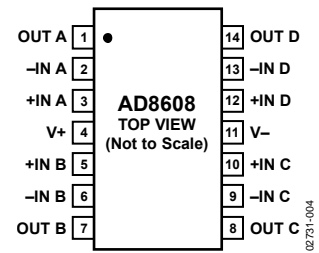


Figure 4. 14-Lead SOIC_N (R Suffix)

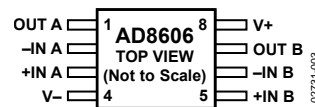


Figure 5. 8-Lead MSOP (RM Suffix),
8-Lead SOIC_N (R Suffix)

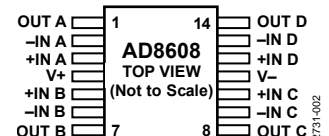


Figure 6. 14-Lead TSSOP (RU Suffix)

TABLE OF CONTENTS

Features	1
Applications	1
General Description	1
Pin Configurations	1
Revision History	2
5 V Electrical Specifications	4
2.7 V Electrical Specifications	6
Absolute Maximum Ratings	8
ESD Caution	8
Typical Performance Characteristics	9
Applications Information	16
Output Phase Reversal	16
Maximum Power Dissipation	16
Input Overvoltage Protection	16

REVISION HISTORY

11/2017—Rev. N to Rev. O

Added Figure 44 and Figure 45; Renumbered Sequentially	15
Changes to Figure 51	17
Changes to Ordering Guide	24

4/2013—Rev. M to Rev. N

Changes to Input Overvoltage Section and THD + Noise Section	16
Changes to Total Noise Including Source Resistors Section	17
Updated Outline Dimensions	24

2/2013—Rev. L to Rev. M

Updated Outline Dimensions	21
Changes to Ordering Guide	24

2/2012—Rev. K to Rev. L

Changed Functional Block Diagrams Section to Pin Configuration Section	1
Changes to Figure 11	9
Added Figure 33	13

8/2011—Rev. J to Rev. K

Changes to Figure 20	2
Updated Outline Dimensions	20
Changes to Ordering Guide	23

8/2010—Rev. I to Rev. J

Changes to Figure 10 and Figure 11	9
Changes to Figure 15	10
Changes to Figure 36	13
Changes to Figure 42	14
Updated Outline Dimensions	20
Changes to Ordering Guide	23

THD + Noise	16
Total Noise Including Source Resistors	17
Channel Separation	17
Capacitive Load Drive	17
Light Sensitivity	18
WLCSP Assembly Considerations	18
I-V Conversion Applications	19
Photodiode Preamplifier Applications	19
Audio and PDA Applications	19
Instrumentation Amplifiers	20
DAC Conversion	20
Outline Dimensions	21
Ordering Guide	24

9/2008—Rev. H to Rev. I

Changes to Input Overvoltage Protection Section	15
Changes to Ordering Guide	22

2/2008—Rev. G to Rev. H

Changes to Features	1
Changes to Table 1	4
Changes to Table 2	6
Changes to Figure 11	9
Changes to Figure 13, Figure 14, and Figure 16 Captions	10
Changes to Figure 15, Figure 17, and Figure 18	10
Changes to Figure 34 and Figure 35 Captions	13
Changes to Figure 36	13
Changes to Figure 37 Caption	14
Changes to Figure 38 and Figure 41	14
Changes to Figure 45	15
Changes to Audio and PDA Applications Section	18
Changes to Figure 52	18
Changes to Ordering Guide	22

10/2007—Rev. F to Rev. G

Changes to Figure 2	1
Updated Outline Dimensions	20

8/2007—Rev. E to Rev. F

Added 8-Ball WLCSP Package	Universal
Changes to Features	1
Changes to Table 1	3
Changes to Table 2	5
Changes to Table 4	7
Updated Outline Dimensions	19
Changes to Ordering Guide	21

1/2006—Rev. D to Rev. E

Changes to Table 1	3
Changes to Table 2	5
Changes to Table 4	6
Changes to Figure 12 Caption	8
Changes to Figure 26 and Figure 27 Captions.....	11
Changes to Figure 33 Caption	12
Changes to Figure 44	14
Updated Outline Dimensions.....	19
Changes to Ordering Guide.....	20

5/2004—Rev. C to Rev. D

Updated Format.....	Universal
Edit to Light Sensitivity Section	16
Updated Outline Dimensions.....	19
Changes to Ordering Guide.....	20

7/2003—Rev. B to Rev. C

Changes to Features	1
Change to General Description.....	1
Addition to Functional Block Diagrams	1
Addition to Absolute Maximum Ratings	4
Addition to Ordering Guide	4
Change to Equation in Maximum Power Dissipation Section	11
Added Light Sensitivity Section	12

Added New Figure 8; Renumbered Subsequently	13
Added New MicroCSP Assembly Considerations Section.....	13
Changes to Figure 9	13
Change to Equation in Photodiode Preamplifier	
Applications Section	13
Changes to Figure 12	14
Change to Equation in D/A Conversion Section.....	14
Updated Outline Dimensions	15

3/2003—Rev. A to Rev. B

Changes to Functional Block Diagram	1
Changes to Absolute Maximum Ratings.....	4
Changes to Ordering Guide	4
Changes to Figure 9	13
Updated Outline Dimensions.....	15

11/2002—Rev. 0 to Rev. A

Change to Electrical Characteristics.....	2
Changes to Absolute Maximum Ratings.....	4
Changes to Ordering Guide	4
Change to TPC 6	5
Updated Outline Dimensions.....	15

5/2002—Revision 0: Initial Version

5 V ELECTRICAL SPECIFICATIONS

$V_S = 5\text{ V}$, $V_{CM} = V_S/2$, $T_A = 25^\circ\text{C}$, unless otherwise noted.

Table 1.

Parameter	Symbol	Conditions	Min	Typ	Max	Unit	
INPUT CHARACTERISTICS							
Offset Voltage	V_{OS}	$V_S = 3.5\text{ V}$, $V_{CM} = 3\text{ V}$ $V_S = 3.5\text{ V}$, $V_{CM} = 2.7\text{ V}$ $V_S = 5\text{ V}$, $V_{CM} = 0\text{ V to } 5\text{ V}$ $-40^\circ\text{C} < T_A < +125^\circ\text{C}$					
AD8605/AD8606 (Except WLCSP)			20	65	μV		
AD8608			20	75	μV		
AD8605/AD8606/AD8608			80	300	μV		
Input Bias Current	I_B	$-40^\circ\text{C} < T_A < +85^\circ\text{C}$ $-40^\circ\text{C} < T_A < +125^\circ\text{C}$ $-40^\circ\text{C} < T_A < +85^\circ\text{C}$ $-40^\circ\text{C} < T_A < +125^\circ\text{C}$		0.2	1	pA	
AD8605/AD8606					50	pA	
AD8605/AD8606						250	pA
AD8608						100	pA
AD8608							300
Input Offset Current	I_{OS}	$-40^\circ\text{C} < T_A < +85^\circ\text{C}$ $-40^\circ\text{C} < T_A < +125^\circ\text{C}$		0.1	0.5	pA	
						20	pA
							75
Input Voltage Range			0		5	V	
Common-Mode Rejection Ratio	CMRR	$V_{CM} = 0\text{ V to } 5\text{ V}$ $-40^\circ\text{C} < T_A < +125^\circ\text{C}$	85	100		dB	
			75	90		dB	
Large Signal Voltage Gain	A_{VO}	$R_L = 2\text{ k}\Omega$, $V_O = 0.5\text{ V to } 4.5\text{ V}$	300	1000		V/mV	
Offset Voltage Drift	$\Delta V_{OS}/\Delta T$	$-40^\circ\text{C} < T_A < +125^\circ\text{C}$ $-40^\circ\text{C} < T_A < +125^\circ\text{C}$		1	4.5	$\mu\text{V}/^\circ\text{C}$	
AD8605/AD8606					1.5	6.0	$\mu\text{V}/^\circ\text{C}$
AD8608						$\mu\text{V}/^\circ\text{C}$	
INPUT CAPACITANCE							
Common-Mode Input Capacitance	C_{COM}			8.8		pF	
Differential Input Capacitance	C_{DIFF}			2.6		pF	
OUTPUT CHARACTERISTICS							
Output Voltage High	V_{OH}	$I_L = 1\text{ mA}$ $I_L = 10\text{ mA}$ $-40^\circ\text{C} < T_A < +125^\circ\text{C}$	4.96	4.98		V	
				4.7	4.79		V
				4.6			V
Output Voltage Low	V_{OL}	$I_L = 1\text{ mA}$ $I_L = 10\text{ mA}$ $-40^\circ\text{C} < T_A < +125^\circ\text{C}$		20	40	mV	
					170	210	mV
						290	mV
Output Current	I_{OUT}			± 80		mA	
Closed-Loop Output Impedance	Z_{OUT}	$f = 1\text{ MHz}$, $A_V = 1$		1		Ω	
POWER SUPPLY							
Power Supply Rejection Ratio	PSRR	$V_S = 2.7\text{ V to } 5.5\text{ V}$ $V_S = 2.7\text{ V to } 5.5\text{ V}$ $V_S = 2.7\text{ V to } 5.5\text{ V}$ $-40^\circ\text{C} < T_A < +125^\circ\text{C}$	80	95		dB	
AD8605/AD8606			75	92		dB	
AD8605/AD8606 WLCSP			77	92		dB	
AD8608			70	90		dB	
Supply Current/Amplifier	I_{SY}	$I_{OUT} = 0\text{ mA}$ $-40^\circ\text{C} < T_A < +125^\circ\text{C}$		1	1.2	mA	
					1.4	mA	
DYNAMIC PERFORMANCE							
Slew Rate	SR	$R_L = 2\text{ k}\Omega$, $C_L = 16\text{ pF}$		5		V/ μs	
Settling Time	t_s	To 0.01%, 0V to 2V step, $A_V = 1$		<1		μs	
Unity Gain Bandwidth Product	GBP			10		MHz	
Phase Margin	Φ_M			65		Degrees	

Parameter	Symbol	Conditions	Min	Typ	Max	Unit
NOISE PERFORMANCE						
Peak-to-Peak Noise	e_n p-p	$f = 0.1 \text{ Hz to } 10 \text{ Hz}$		2.3	3.5	$\mu\text{V p-p}$
Voltage Noise Density	e_n	$f = 1 \text{ kHz}$		8	12	$\text{nV}/\sqrt{\text{Hz}}$
	e_n	$f = 10 \text{ kHz}$		6.5		$\text{nV}/\sqrt{\text{Hz}}$
Current Noise Density	i_n	$f = 1 \text{ kHz}$		0.01		$\text{pA}/\sqrt{\text{Hz}}$

2.7 V ELECTRICAL SPECIFICATIONS

$V_S = 2.7\text{ V}$, $V_{CM} = V_S/2$, $T_A = 25^\circ\text{C}$, unless otherwise noted.

Table 2.

Parameter	Symbol	Conditions	Min	Typ	Max	Unit
INPUT CHARACTERISTICS						
Offset Voltage	V_{OS}					
AD8605/AD8606 (Except WLCSP)		$V_S = 3.5\text{ V}$, $V_{CM} = 3\text{ V}$		20	65	μV
AD8608		$V_S = 3.5\text{ V}$, $V_{CM} = 2.7\text{ V}$		20	75	μV
AD8605/AD8606/AD8608		$V_S = 2.7\text{ V}$, $V_{CM} = 0\text{ V to } 2.7\text{ V}$ $-40^\circ\text{C} < T_A < +125^\circ\text{C}$		80	300	μV
					750	μV
Input Bias Current	I_B			0.2	1	pA
AD8605/AD8606		$-40^\circ\text{C} < T_A < +85^\circ\text{C}$			50	pA
AD8605/AD8606		$-40^\circ\text{C} < T_A < +125^\circ\text{C}$			250	pA
AD8608		$-40^\circ\text{C} < T_A < +85^\circ\text{C}$			100	pA
AD8608		$-40^\circ\text{C} < T_A < +125^\circ\text{C}$			300	pA
Input Offset Current	I_{OS}			0.1	0.5	pA
		$-40^\circ\text{C} < T_A < +85^\circ\text{C}$			20	pA
		$-40^\circ\text{C} < T_A < +125^\circ\text{C}$			75	pA
Input Voltage Range			0		2.7	V
Common-Mode Rejection Ratio	CMRR	$V_{CM} = 0\text{ V to } 2.7\text{ V}$ $-40^\circ\text{C} < T_A < +125^\circ\text{C}$	80	95		dB
			70	85		dB
Large Signal Voltage Gain	A_{VO}	$R_L = 2\text{ k}\Omega$, $V_O = 0.5\text{ V to } 2.2\text{ V}$	110	350		V/mV
Offset Voltage Drift						
AD8605/AD8606	$\Delta V_{OS}/\Delta T$	$-40^\circ\text{C} < T_A < +125^\circ\text{C}$		1	4.5	$\mu\text{V}/^\circ\text{C}$
AD8608	$\Delta V_{OS}/\Delta T$	$-40^\circ\text{C} < T_A < +125^\circ\text{C}$		1.5	6.0	$\mu\text{V}/^\circ\text{C}$
INPUT CAPACITANCE						
Common-Mode Input Capacitance	C_{COM}			8.8		pF
Differential Input Capacitance	C_{DIFF}			2.6		pF
OUTPUT CHARACTERISTICS						
Output Voltage High	V_{OH}	$I_L = 1\text{ mA}$ $-40^\circ\text{C} < T_A < +125^\circ\text{C}$	2.6	2.66		V
			2.6			V
Output Voltage Low	V_{OL}	$I_L = 1\text{ mA}$ $-40^\circ\text{C} < T_A < +125^\circ\text{C}$		25	40	mV
					50	mV
Output Current	I_{OUT}			± 30		mA
Closed-Loop Output Impedance	Z_{OUT}	$f = 1\text{ MHz}$, $A_V = 1$		1.2		Ω
POWER SUPPLY						
Power Supply Rejection Ratio	PSRR					
AD8605/AD8606		$V_S = 2.7\text{ V to } 5.5\text{ V}$	80	95		dB
AD8605/AD8606 WLCSP		$V_S = 2.7\text{ V to } 5.5\text{ V}$	75	92		dB
AD8608		$V_S = 2.7\text{ V to } 5.5\text{ V}$ $-40^\circ\text{C} < T_A < +125^\circ\text{C}$	77	92		dB
			70	90		dB
Supply Current/Amplifier	I_{SY}	$I_{OUT} = 0\text{ mA}$ $-40^\circ\text{C} < T_A < +125^\circ\text{C}$		1.15	1.4	mA
					1.5	mA
DYNAMIC PERFORMANCE						
Slew Rate	SR	$R_L = 2\text{ k}\Omega$, $C_L = 16\text{ pF}$		5		V/ μs
Settling Time	t_s	To 0.01%, 0V to 1V step, $A_V = 1$		<0.5		μs
Unity Gain Bandwidth Product	GBP			9		MHz
Phase Margin	Φ_M			50		Degrees

Parameter	Symbol	Conditions	Min	Typ	Max	Unit
NOISE PERFORMANCE						
Peak-to-Peak Noise	e_n p-p	$f = 0.1 \text{ Hz to } 10 \text{ Hz}$		2.3	3.5	$\mu\text{V p-p}$
Voltage Noise Density	e_n	$f = 1 \text{ kHz}$		8	12	$\text{nV}/\sqrt{\text{Hz}}$
	e_n	$f = 10 \text{ kHz}$		6.5		$\text{nV}/\sqrt{\text{Hz}}$
Current Noise Density	i_n	$f = 1 \text{ kHz}$		0.01		$\text{pA}/\sqrt{\text{Hz}}$

ABSOLUTE MAXIMUM RATINGS

Table 3.

Parameter	Rating
Supply Voltage	6 V
Input Voltage	GND to V_S
Differential Input Voltage	6 V
Output Short-Circuit Duration to GND	Observe Derating Curves
Storage Temperature Range	
All Packages	−65°C to +150°C
Operating Temperature Range	
All Packages	−40°C to +125°C
Junction Temperature Range	
All Packages	−65°C to +150°C
Lead Temperature (Soldering, 60 sec)	300°C

Stresses at or above those listed under Absolute Maximum Ratings may cause permanent damage to the product. This is a stress rating only; functional operation of the product at these or any other conditions above those indicated in the operational section of this specification is not implied. Operation beyond the maximum operating conditions for extended periods may affect product reliability.

Table 4.

Package Type	θ_{JA}^1	θ_{JC}	Unit
5-Ball WLCSP (CB)	170		°C/W
5-Lead SOT-23 (RJ)	240	92	°C/W
8-Ball WLCSP (CB)	115		°C/W
8-Lead MSOP (RM)	206	44	°C/W
8-Lead SOIC_N (R)	157	56	°C/W
14-Lead SOIC_N (R)	105	36	°C/W
14-Lead TSSOP (RU)	148	23	°C/W

¹ θ_{JA} is specified for the worst-case conditions, that is, a device soldered in a circuit board for surface-mount packages.

ESD CAUTION



ESD (electrostatic discharge) sensitive device. Charged devices and circuit boards can discharge without detection. Although this product features patented or proprietary protection circuitry, damage may occur on devices subjected to high energy ESD. Therefore, proper ESD precautions should be taken to avoid performance degradation or loss of functionality.

TYPICAL PERFORMANCE CHARACTERISTICS

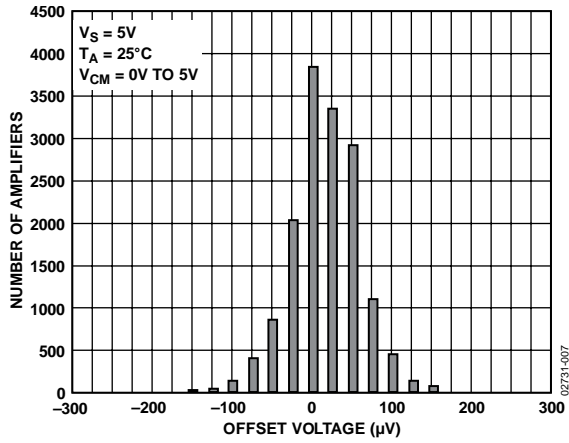


Figure 7. Input Offset Voltage Distribution

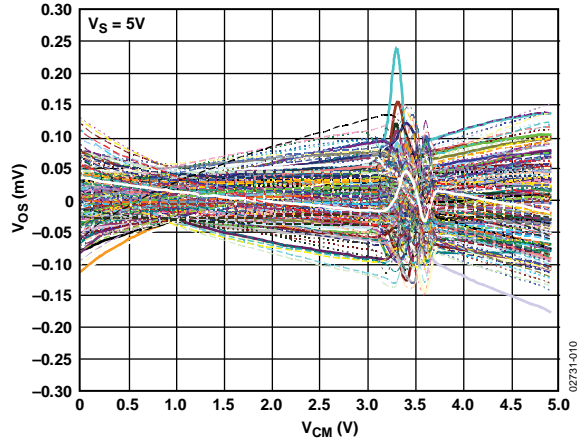


Figure 10. Input Offset Voltage vs. Common-Mode Voltage (200 Units, 5 Wafer Lots, Including Process Skews)

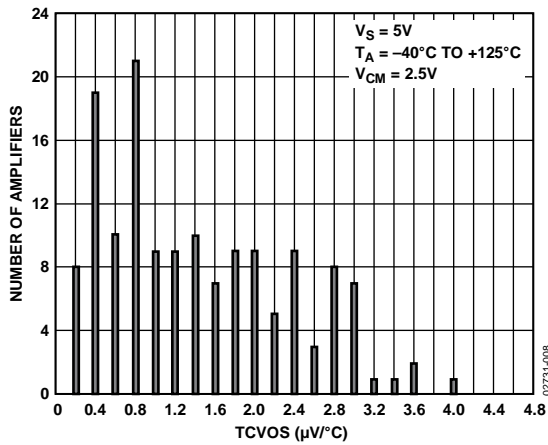


Figure 8. AD8608 Input Offset Voltage Drift Distribution

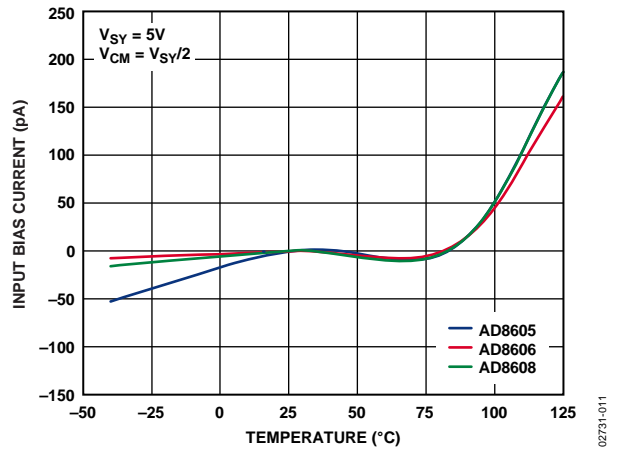


Figure 11. Input Bias Current vs. Temperature

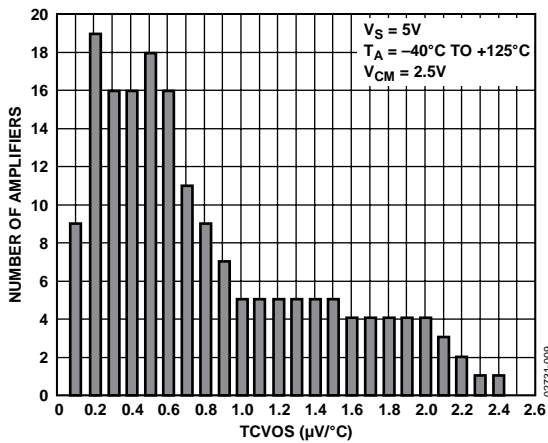


Figure 9. AD8605/AD8606 Input Offset Voltage Drift Distribution

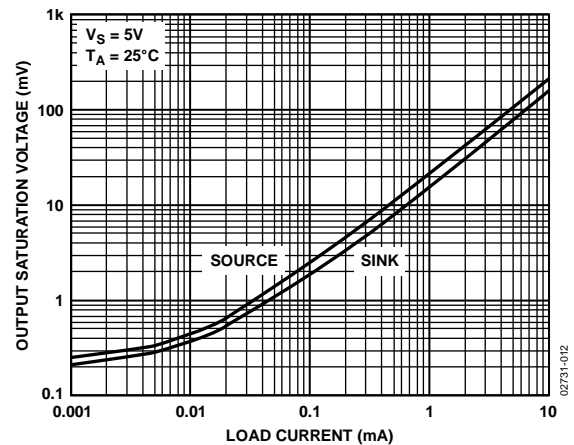


Figure 12. Output Saturation Voltage vs. Load Current

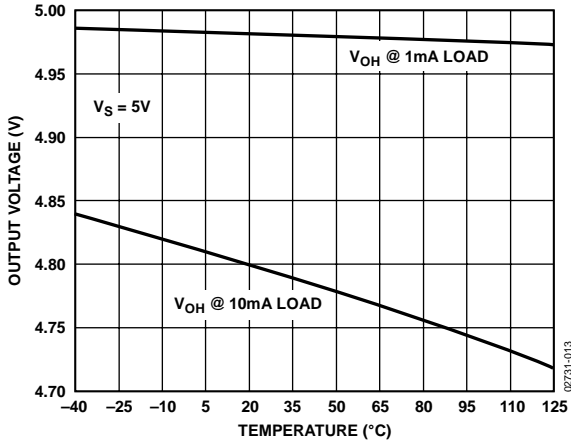


Figure 13. Output Voltage Swing High vs. Temperature

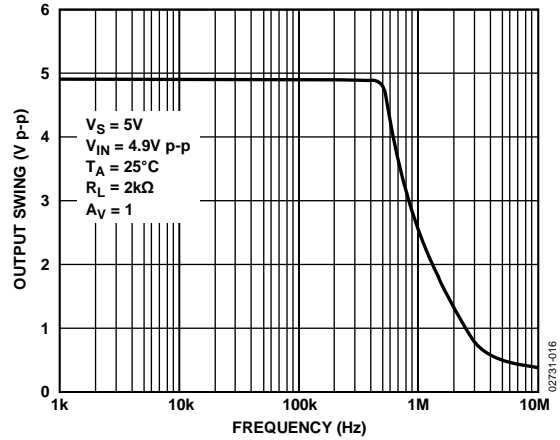


Figure 16. Closed-Loop Output Voltage Swing (FPBW)

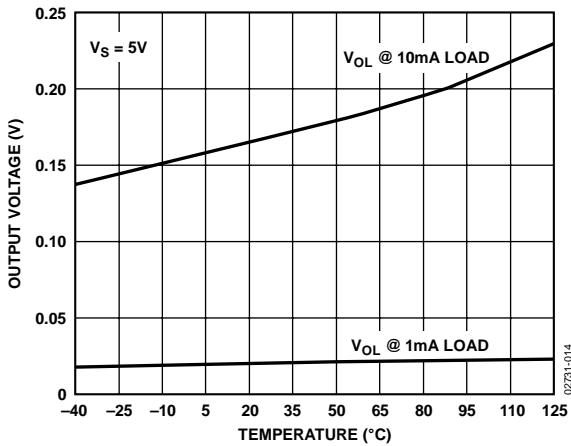


Figure 14. Output Voltage Swing Low vs. Temperature

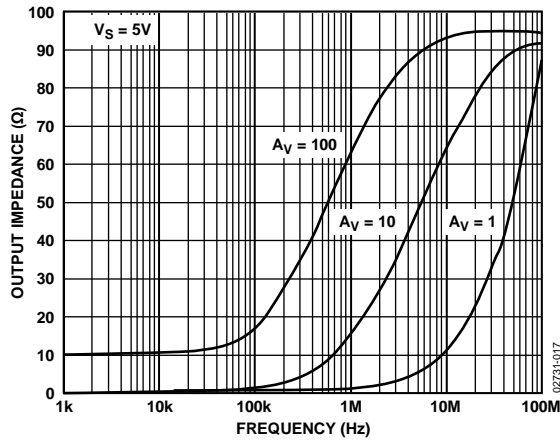


Figure 17. Output Impedance vs. Frequency

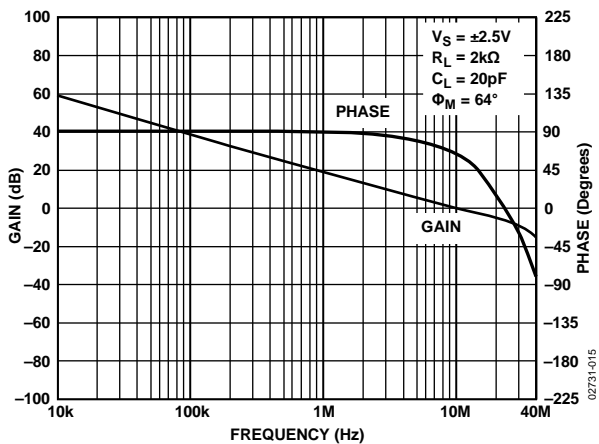


Figure 15. Open-Loop Gain and Phase vs. Frequency

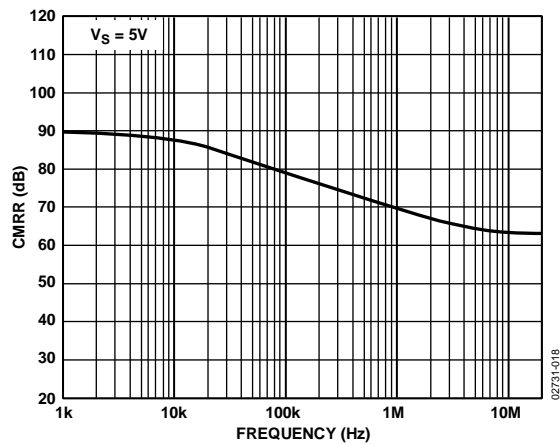


Figure 18. Common-Mode Rejection Ratio (CMRR) vs. Frequency

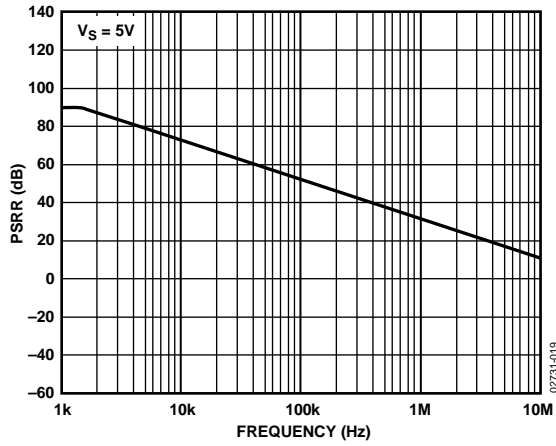


Figure 19. PSRR vs. Frequency

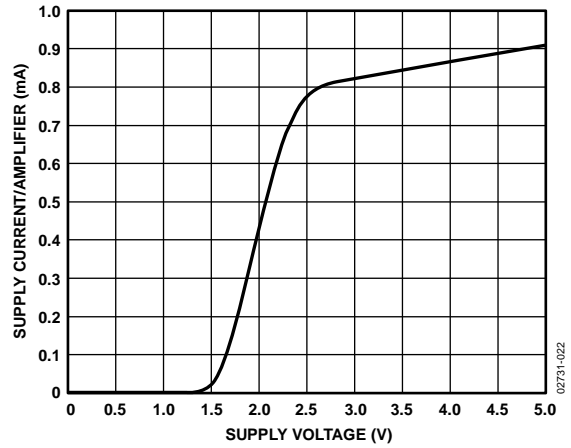


Figure 22. Supply Current/Amplifier vs. Supply Voltage

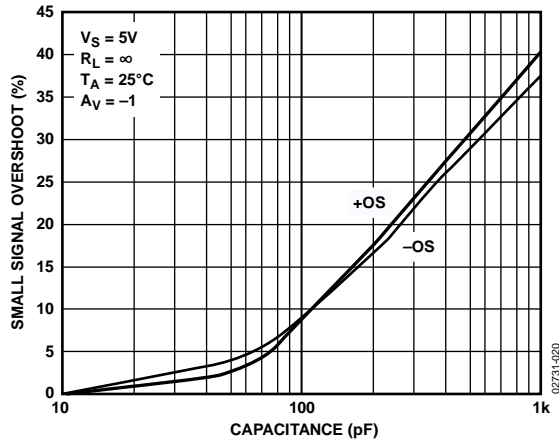


Figure 20. Small Signal Overshoot vs. Load Capacitance

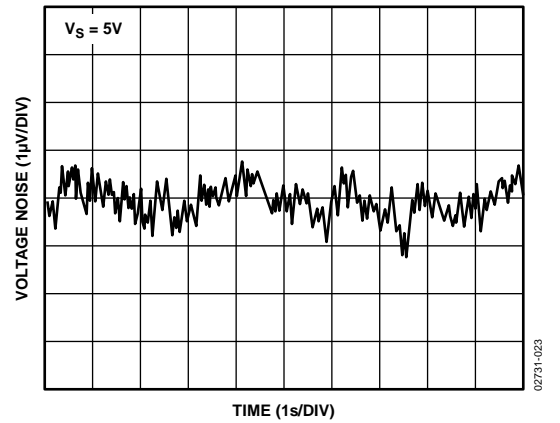


Figure 23. 0.1 Hz to 10 Hz Input Voltage Noise

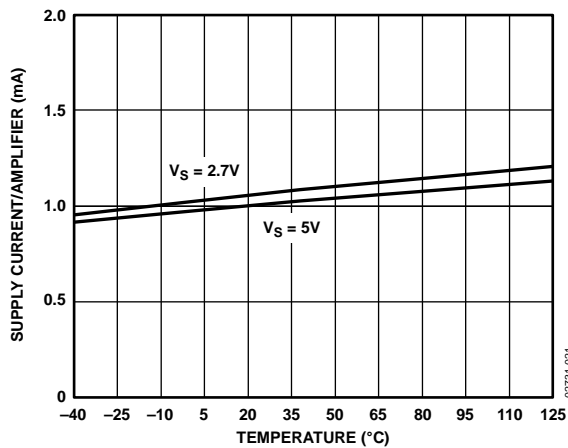


Figure 21. Supply Current/Amplifier vs. Temperature

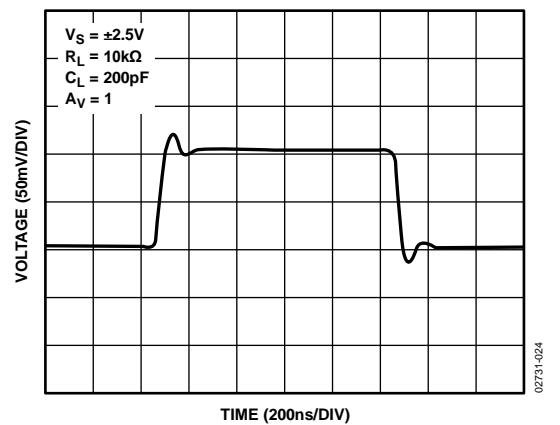


Figure 24. Small Signal Transient Response

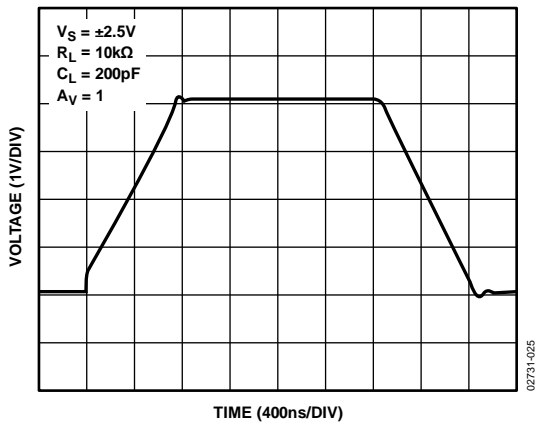


Figure 25. Large Signal Transient Response

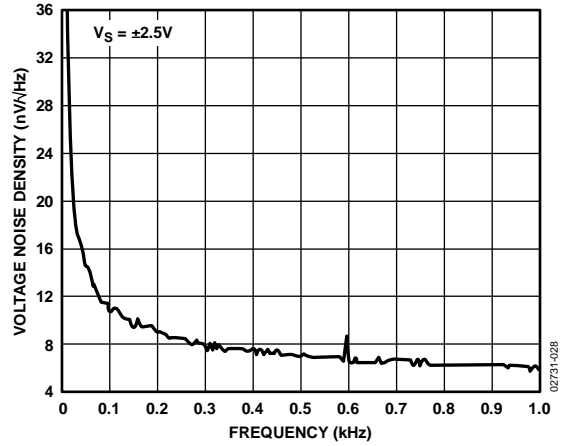


Figure 28. Voltage Noise Density vs. Frequency

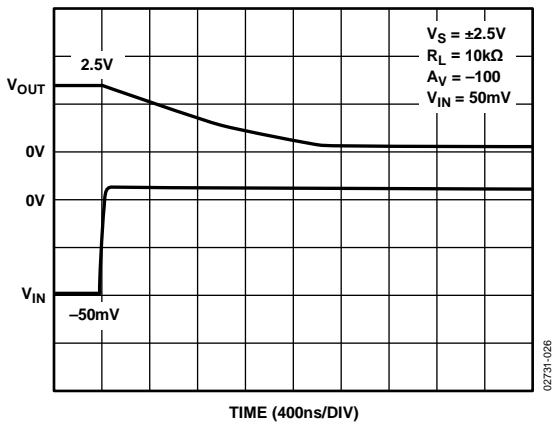


Figure 26. Positive Overload Recovery

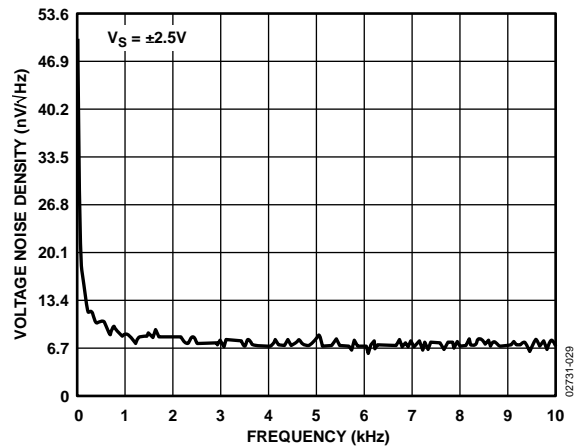


Figure 29. Voltage Noise Density vs. Frequency

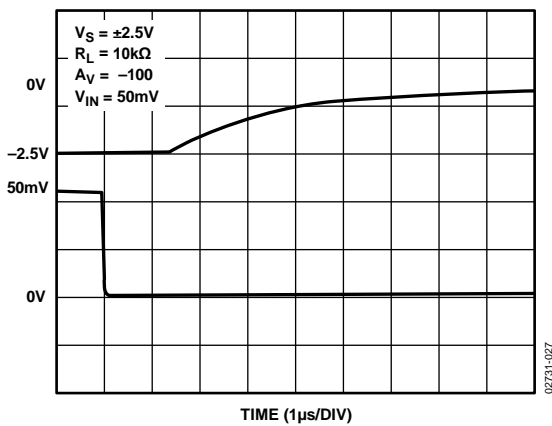


Figure 27. Negative Overload Recovery

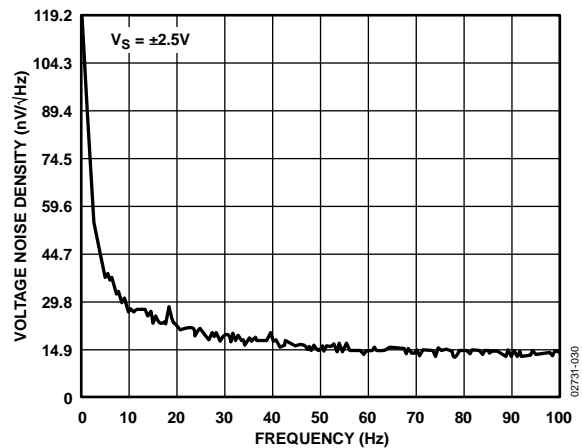


Figure 30. Voltage Noise Density vs. Frequency

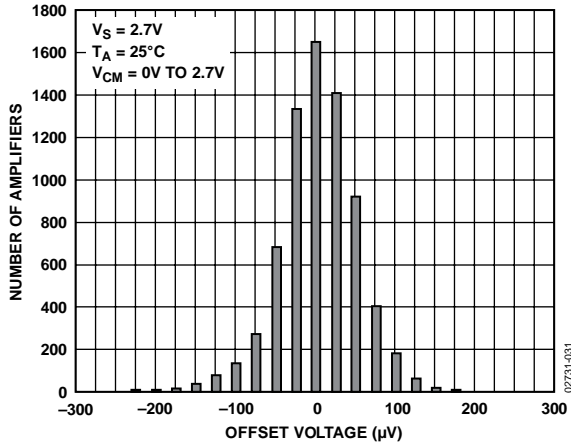


Figure 31. Input Offset Voltage Distribution

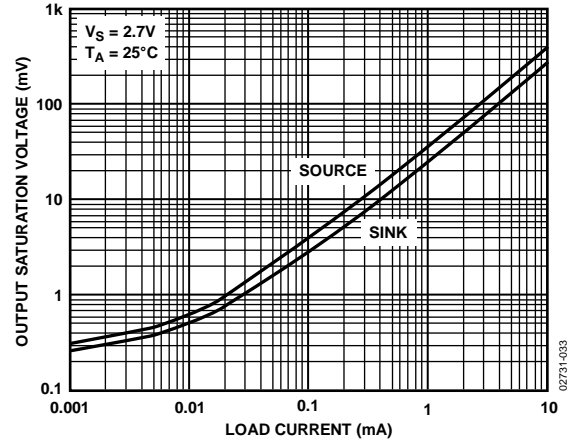


Figure 34. Output Saturation Voltage vs. Load Current

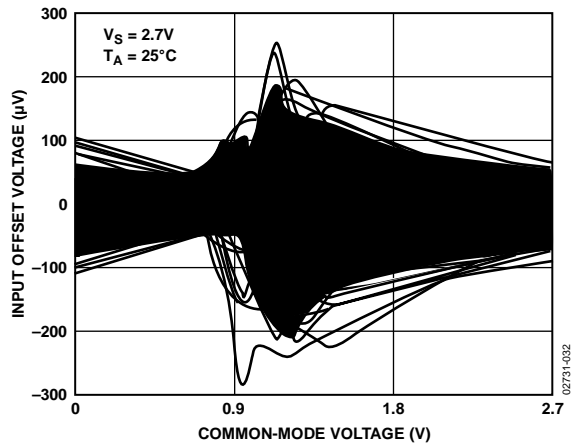


Figure 32. Input Offset Voltage vs. Common-Mode Voltage (200 Units, 5 Wafer Lots, Including Process Skews)

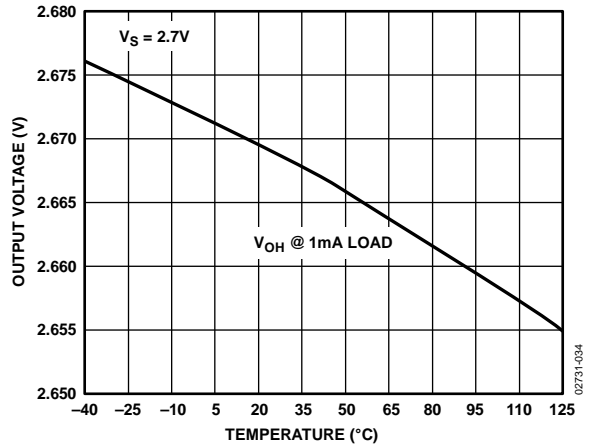


Figure 35. Output Voltage Swing High vs. Temperature

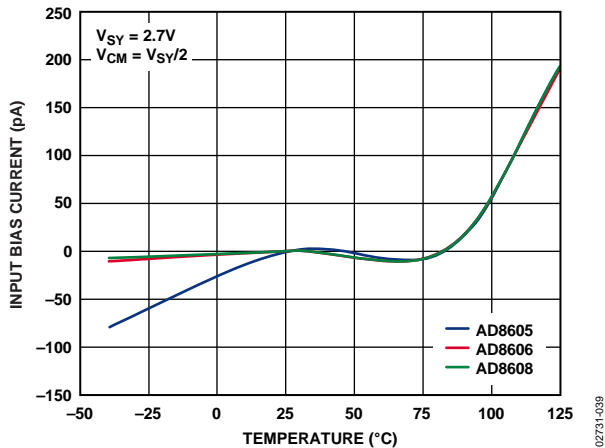


Figure 33. Input Bias Current vs. Temperature

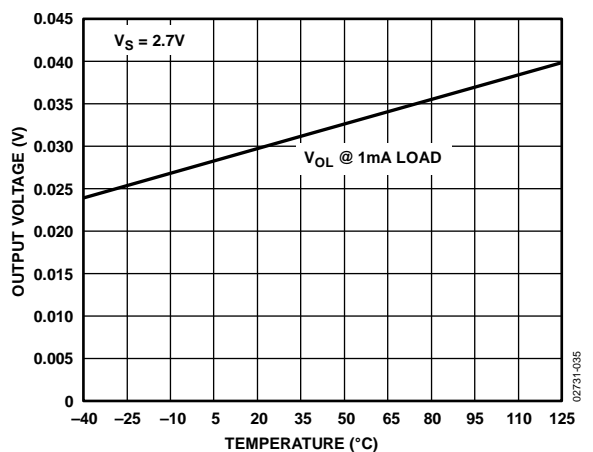


Figure 36. Output Voltage Swing Low vs. Temperature

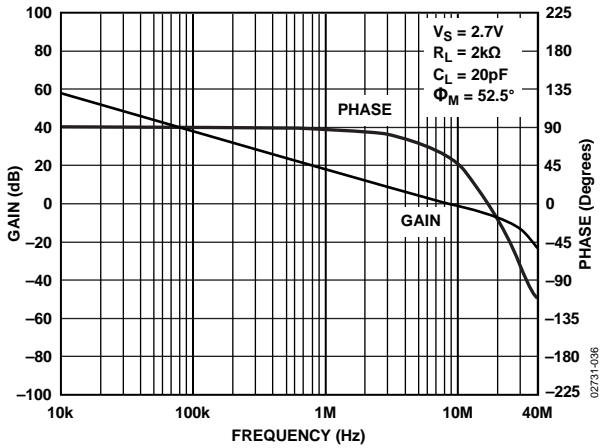


Figure 37. Open-Loop Gain and Phase vs. Frequency

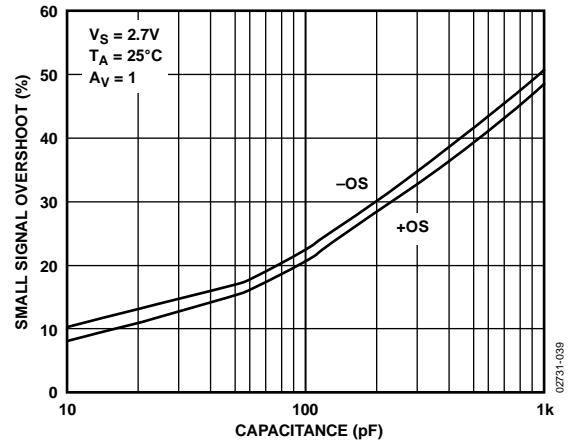


Figure 40. Small Signal Overshoot vs. Load Capacitance

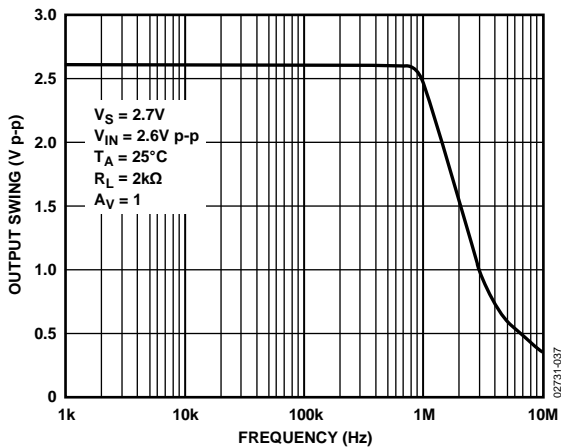


Figure 38. Closed-Loop Output Voltage Swing vs. Frequency (FPBW)

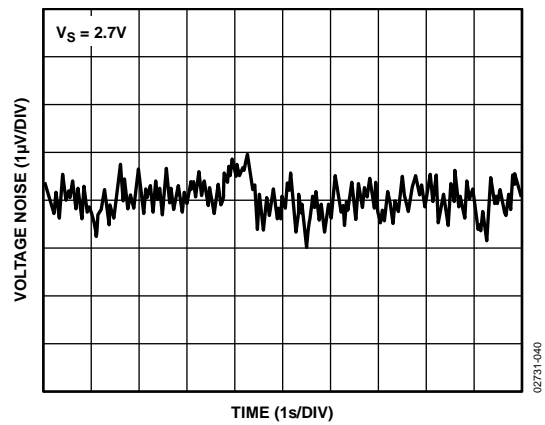


Figure 41. 0.1 Hz to 10 Hz Input Voltage Noise

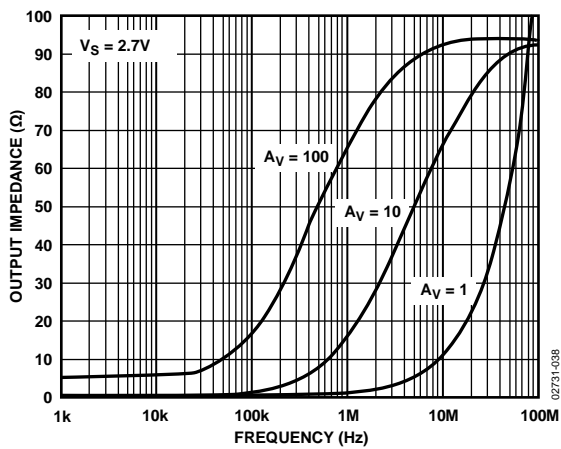


Figure 39. Output Impedance vs. Frequency

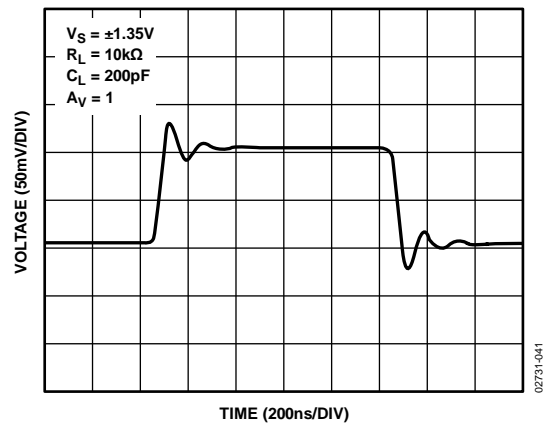


Figure 42. Small Signal Transient Response

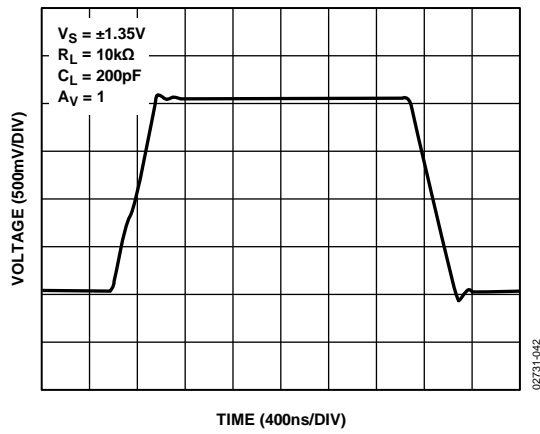


Figure 43. Large Signal Transient Response

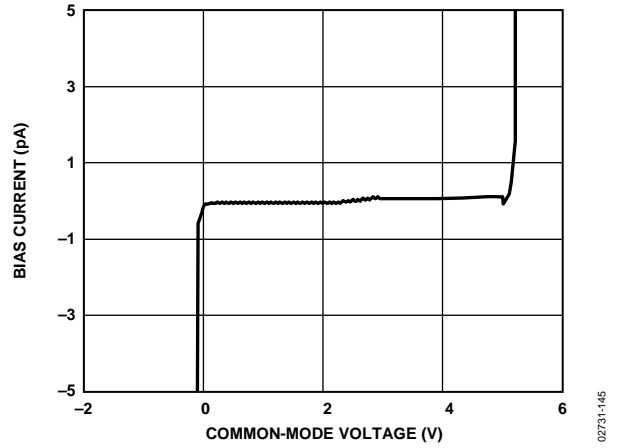


Figure 45. Noninverting Input Bias Current vs Common-Mode Voltage

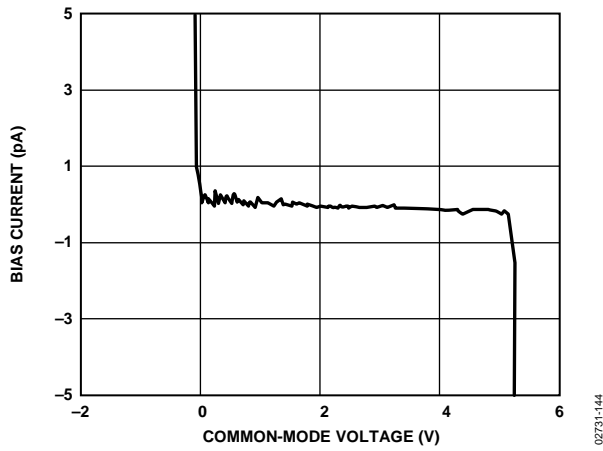


Figure 44. Inverting Input Bias Current vs Common-Mode Voltage

APPLICATIONS INFORMATION

OUTPUT PHASE REVERSAL

Phase reversal is defined as a change in polarity at the output of the amplifier when a voltage that exceeds the maximum input common-mode voltage drives the input.

Phase reversal can cause permanent damage to the amplifier; it can also cause system lockups in feedback loops. The AD8605 does not exhibit phase reversal even for inputs exceeding the supply voltage by more than 2 V.

MAXIMUM POWER DISSIPATION

Power dissipated in an IC causes the die temperature to increase, which can affect the behavior of the IC and the application circuit performance.

The absolute maximum junction temperature of the AD8605/AD8606/AD8608 is 150°C. Exceeding this temperature could damage or destroy the device.

The maximum power dissipation of the amplifier is calculated according to

$$P_{DISS} = \frac{T_J - T_A}{\theta_{JA}}$$

where:

T_J is the junction temperature.

T_A is the ambient temperature.

θ_{JA} is the junction-to-ambient thermal resistance.

Figure 47 compares the maximum power dissipation with temperature for the various AD860x family packages.

INPUT OVERVOLTAGE PROTECTION

The AD860x has internal protective circuitry. However, if the voltage applied at either input exceeds the supplies by more than 0.5 V, external resistors should be placed in series with the inputs. The resistor values can be determined by

$$\frac{V_{IN} - V_S}{R_S} \leq 5 \text{ mA}$$

The remarkable low input offset current of the AD860x (<1 pA) allows the use of larger value resistors. With a 10 kΩ resistor at the input, the output voltage has less than 10 nV of error voltage. A 10 kΩ resistor has less than 13 nV/√Hz of thermal noise at room temperature.

THD + NOISE

Total harmonic distortion is the ratio of the input signal in V rms to the total harmonics in V rms throughout the spectrum. Harmonic distortion adds errors to precision measurements and adds unpleasant sonic artifacts to audio systems.

The AD860x has a low total harmonic distortion. Figure 48 shows that the AD8605 has less than 0.005% or -86 dB of THD + N over the entire audio frequency range. The AD8605 is configured in positive unity gain, which is the worst case, and with a load of 10 kΩ.

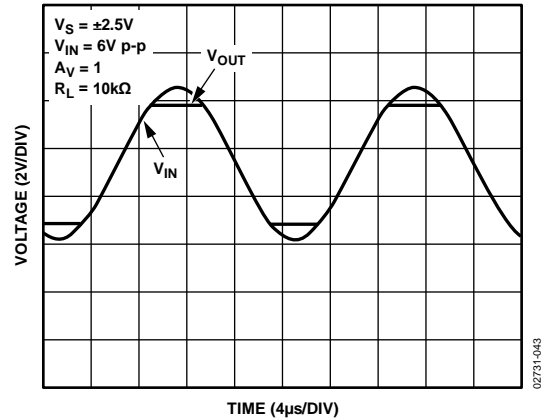


Figure 46. No Phase Reversal

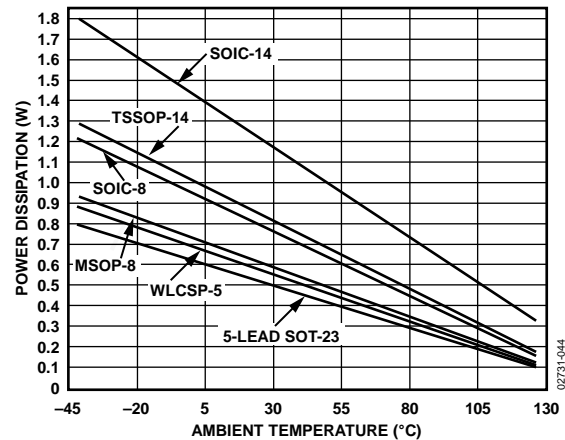


Figure 47. Maximum Power Dissipation vs. Ambient Temperature

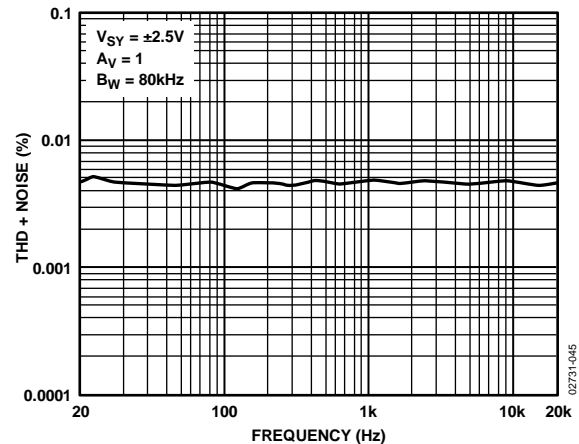


Figure 48. THD + Noise vs. Frequency

TOTAL NOISE INCLUDING SOURCE RESISTORS

The low input current noise and input bias current of the AD860x make it the ideal amplifier for circuits with substantial input source resistance, such as photodiodes. Input offset voltage increases by less than 0.5 nV per 1 kΩ of source resistance at room temperature and increases to 10 nV at 85°C. The total noise density of the circuit is

$$e_{n,TOTAL} = \sqrt{e_n^2 + (i_n R_s)^2 + 4kTR_s}$$

where:

e_n is the input voltage noise density of the AD860x.

i_n is the input current noise density of the AD860x.

R_s is the source resistance at the noninverting terminal.

k is Boltzmann's constant (1.38×10^{-23} J/K).

T is the ambient temperature in Kelvin ($T = 273 + ^\circ\text{C}$).

For example, with $R_s = 10$ kΩ, the total voltage noise density is roughly 15 nV/ $\sqrt{\text{Hz}}$.

For $R_s < 3.9$ kΩ, e_n dominates and $e_{n,TOTAL} \approx e_n$.

The current noise of the AD860x is so low that its total density does not become a significant term unless R_s is greater than 6 MΩ.

The total equivalent rms noise over a specific bandwidth is expressed as

$$E_n = (e_{n,TOTAL}) \sqrt{BW}$$

where BW is the bandwidth in hertz.

Note that the previous analysis is valid for frequencies greater than 100 Hz and assumes relatively flat noise, above 10 kHz. For lower frequencies, flicker noise ($1/f$) must be considered.

CHANNEL SEPARATION

Channel separation, or inverse crosstalk, is a measure of the signal feed from one amplifier (channel) to another on the same IC.

The AD8606 has a channel separation of greater than -160 dB up to frequencies of 1 MHz, allowing the two amplifiers to amplify ac signals independently in most applications.

CAPACITIVE LOAD DRIVE

The AD860x can drive large capacitive loads without oscillation. Figure 50 shows the output of the AD8606 in response to a 200 mV input signal. In this case, the amplifier is configured in positive unity gain, worst case for stability, while driving a 1000 pF load at its output. Driving larger capacitive loads in unity gain can require the use of additional circuitry.

A snubber network, shown in Figure 51, helps reduce the signal overshoot to a minimum and maintain stability. Although this circuit does not recover the loss of bandwidth induced by large capacitive loads, it greatly reduces the overshoot and ringing. This method does not reduce the maximum output swing of the amplifier.

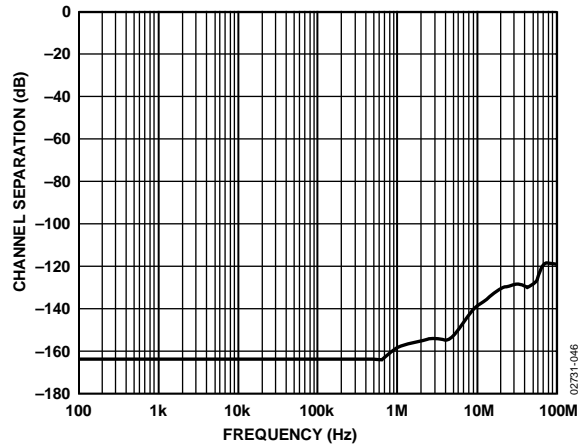


Figure 49. Channel Separation vs. Frequency

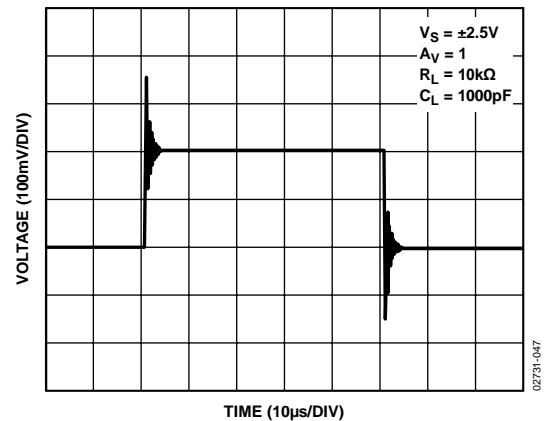


Figure 50. AD8606 Capacitive Load Drive Without Snubber

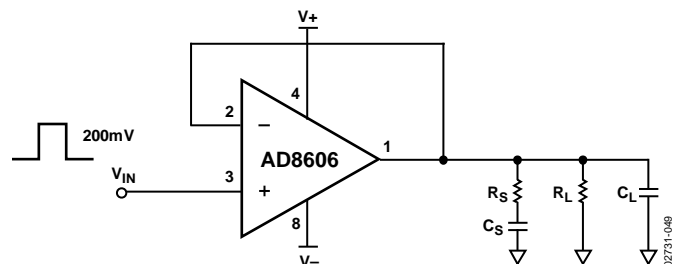


Figure 51. Snubber Network Configuration

Figure 52 shows a scope of the output at the snubber circuit. The overshoot is reduced from over 70% to less than 5%, and the ringing is eliminated by the snubber. Optimum values for R_s and C_s are determined experimentally.

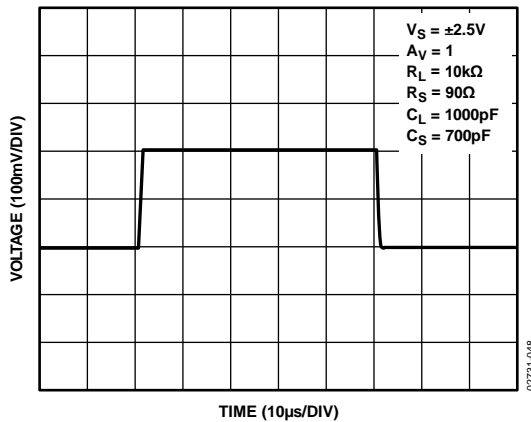


Figure 52. Capacitive Load Drive with Snubber

Table 5 summarizes a few optimum values for capacitive loads.

Table 5.

C_L (pF)	R_s (Ω)	C_s (pF)
500	100	1000
1000	70	1000
2000	60	800

An alternate technique is to insert a series resistor inside the feedback loop at the output of the amplifier. Typically, the value of this resistor is approximately 100 Ω . This method also reduces overshoot and ringing but causes a reduction in the maximum output swing.

LIGHT SENSITIVITY

The AD8605ACB (WLCSP package option) is essentially a silicon die with additional postfabrication dielectric and intermetallic processing designed to contact solder bumps on the active side of the chip. With this package type, the die is exposed to ambient light and is subject to photoelectric effects. Light sensitivity analysis of the AD8605ACB mounted on standard PCB material reveals that only the input bias current (I_B) parameter is impacted when the package is illuminated directly by high intensity light. No degradation in electrical performance is observed due to illumination by low intensity (0.1 mW/cm²) ambient light. Figure 53 shows that I_B increases with increasing wavelength and intensity of incident light; I_B can reach levels as high as 4500 pA at a light intensity of 3 mW/cm² and a wavelength of 850 nm. The light intensities shown in Figure 53 are not normal for most applications, that is, even though direct sunlight can have intensities of 50 mW/cm², office ambient light can be as low as 0.1 mW/cm².

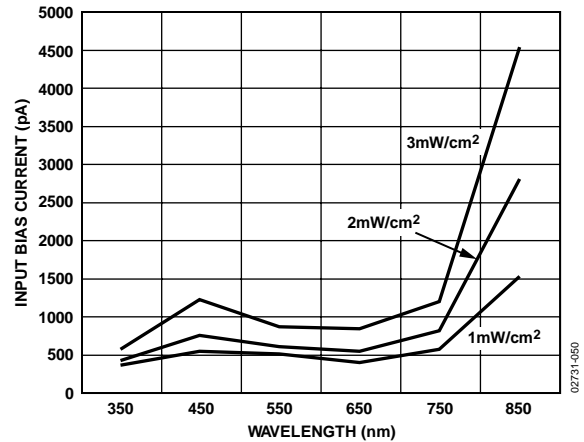


Figure 53. AD8605ACB Input Bias Current Response to Direct Illumination of Varying Intensity and Wavelength

When the WLCSP package is assembled on the board with the bump side of the die facing the PCB, reflected light from the PCB surface is incident on active silicon circuit areas and results in the increased I_B . No performance degradation occurs due to illumination of the backside (substrate) of the AD8605ACB. The AD8605ACB is particularly sensitive to incident light with wavelengths in the near infrared range (NIR, 700 nm to 1000 nm). Photons in this waveband have a longer wavelength and lower energy than photons in the visible (400 nm to 700 nm) and near ultraviolet (NUV, 200 nm to 400 nm) bands; therefore, they can penetrate more deeply into the active silicon. Incident light with wavelengths greater than 1100 nm has no photoelectric effect on the AD8605ACB because silicon is transparent to wavelengths in this range. The spectral content of conventional light sources varies. Sunlight has a broad spectral range, with peak intensity in the visible band that falls off in the NUV and NIR bands; fluorescent lamps have significant peaks in the visible but not the NUV or NIR bands.

Efforts have been made at a product level to reduce the effect of ambient light; the under bump metal (UBM) has been designed to shield the sensitive circuit areas on the active side (bump side) of the die. However, if an application encounters any light sensitivity with the AD8605ACB, shielding the bump side of the WLCSP package with opaque material should eliminate this effect. Shielding can be accomplished using materials such as silica-filled liquid epoxies that are used in flip-chip underfill techniques.

WLCSP ASSEMBLY CONSIDERATIONS

For detailed information on the WLCSP PCB assembly and reliability, see Application Note AN-617, *MicroCSP™ Wafer Level Chip Scale Package*.

I-V CONVERSION APPLICATIONS

PHOTODIODE PREAMPLIFIER APPLICATIONS

The low offset voltage and input current of the AD8605 make it an excellent choice for photodiode applications. In addition, the low voltage and current noise make the amplifier ideal for application circuits with high sensitivity.

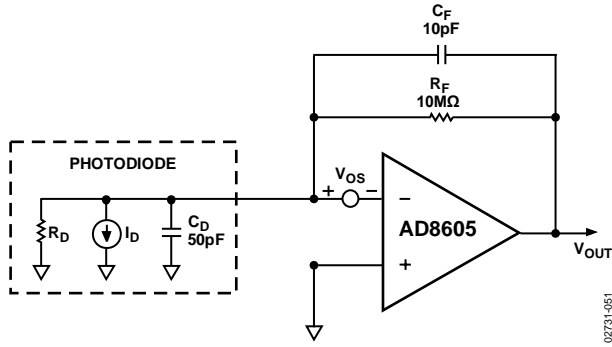


Figure 54. Equivalent Circuit for Photodiode Preamp

The input bias current of the amplifier contributes an error term that is proportional to the value of R_F .

The offset voltage causes a dark current induced by the shunt resistance of the Diode R_D . These error terms are combined at the output of the amplifier. The error voltage is written as

$$E_O = V_{OS} \left(1 + \frac{R_F}{R_D} \right) + R_F I_B$$

Typically, R_F is smaller than R_D , thus R_F/R_D can be ignored.

At room temperature, the AD8605 has an input bias current of 0.2 pA and an offset voltage of 100 μ V. Typical values of R_D are in the range of 1 G Ω .

For the circuit shown in Figure 54, the output error voltage is approximately 100 μ V at room temperature, increasing to about 1 mV at 85°C.

The maximum achievable signal bandwidth is

$$f_{MAX} = \sqrt{\frac{f_t}{2\pi R_F C_F}}$$

where f_t is the unity gain frequency of the amplifier.

AUDIO AND PDA APPLICATIONS

The low distortion and wide dynamic range of the AD860x make it a great choice for audio and PDA applications, including microphone amplification and line output buffering.

Figure 55 shows a typical application circuit for headphone/line-out amplification.

$R1$ and $R2$ are used to bias the input voltage at half the supply, which maximizes the signal bandwidth range. $C1$ and $C2$ are used to ac couple the input signal. $C1$, $R1$, and $R2$ form a high-pass filter whose corner frequency is $1/[2\pi(R1||R2)C1]$.

The high output current of the AD8606 allows it to drive heavy resistive loads.

The circuit in Figure 55 is tested to drive a 16 Ω headphone. The THD + N is maintained at approximately -60 dB throughout the audio range.

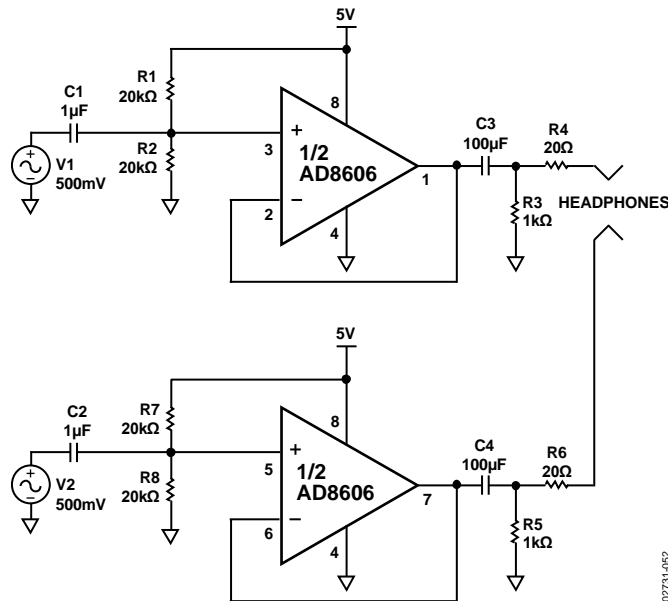


Figure 55. Single-Supply Headphone/Speaker Amplifier

INSTRUMENTATION AMPLIFIERS

The low offset voltage and low noise of the AD8605 make it an ideal amplifier for instrumentation applications.

Difference amplifiers are widely used in high accuracy circuits to improve the common-mode rejection ratio. Figure 56 shows a simple difference amplifier. Figure 57 shows the common-mode rejection for a unity gain configuration and for a gain of 10.

Making $(R4/R3) = (R2/R1)$ and choosing 0.01% tolerance yields a CMRR of 74 dB and minimizes the gain error at the output.

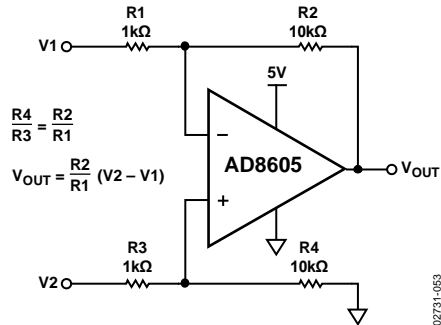


Figure 56. Difference Amplifier, $A_v = 10$

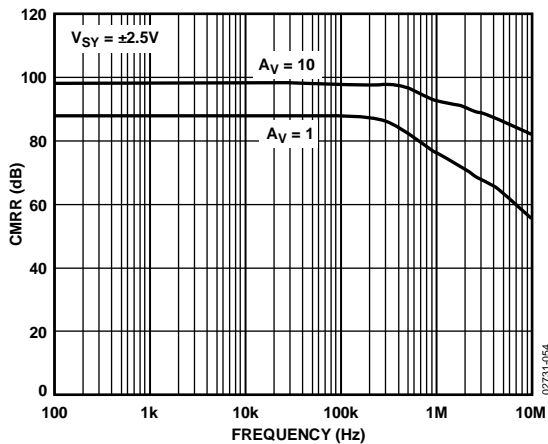


Figure 57. Difference Amplifier CMRR vs. Frequency

DAC CONVERSION

The low input bias current and offset voltage of the AD8605 make it an excellent choice for buffering the output of a current output DAC.

Figure 58 shows a typical implementation of the AD8605 at the output of a 12-bit DAC.

The DAC8143 output current is converted to a voltage by the feedback resistor. The equivalent resistance at the output of the DAC varies with the input code, as does the output capacitance.

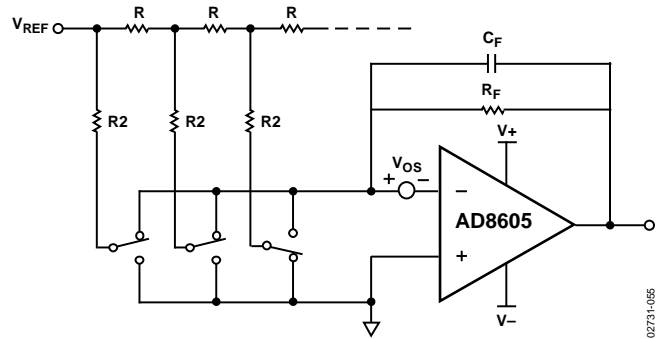


Figure 58. Simplified Circuit of the DAC8143 with AD8605 Output Buffer

To optimize the performance of the DAC, insert a capacitor in the feedback loop of the AD8605 to compensate the amplifier for the pole introduced by the output capacitance of the DAC. Typical values for C_F range from 10 pF to 30 pF; it can be adjusted for the best frequency response. The total error at the output of the op amp can be computed by

$$E_o = V_{os} \left(1 + \frac{R_F}{Req} \right)$$

where Req is the equivalent resistance seen at the output of the DAC. As previously mentioned, Req is code dependent and varies with the input. A typical value for Req is 15 kΩ. Choosing a feedback resistor of 10 kΩ yields an error of less than 200 μV.

Figure 59 shows the implementation of a dual-stage buffer at the output of a DAC. The first stage is used as a buffer. Capacitor C1 with Req creates a low-pass filter, and thus, provides phase lead to compensate for frequency response. The second stage of the AD8606 is used to provide voltage gain at the output of the buffer.

Grounding the positive input terminals in both stages reduces errors due to the common-mode output voltage. Choosing R1, R2, and R3 to match within 0.01% yields a CMRR of 74 dB and maintains minimum gain error in the circuit.

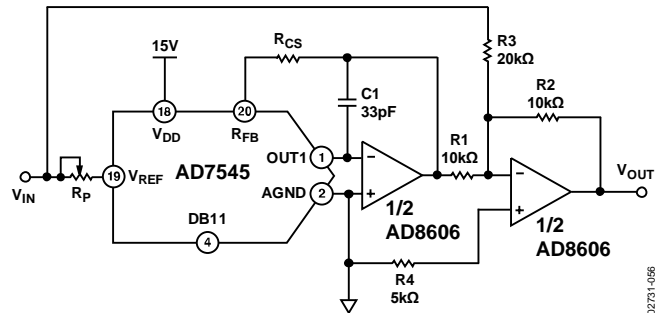


Figure 59. Bipolar Operation

OUTLINE DIMENSIONS

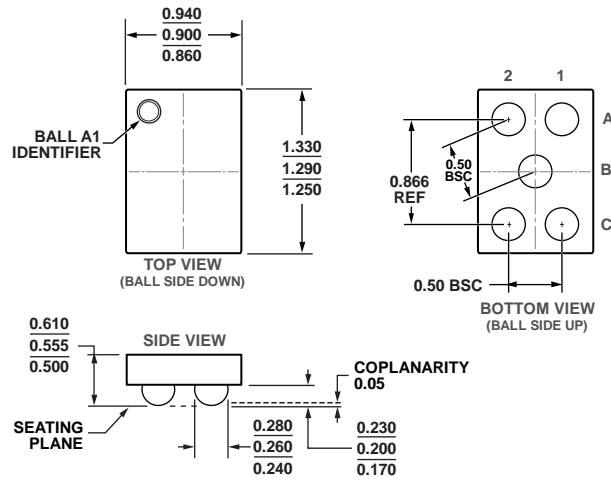
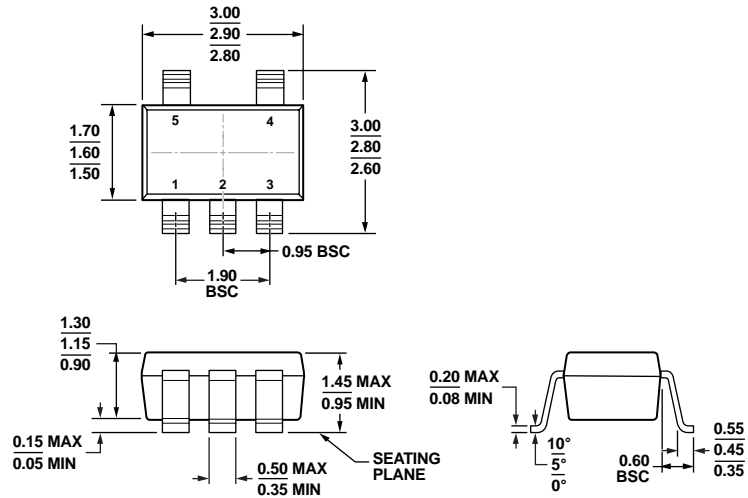


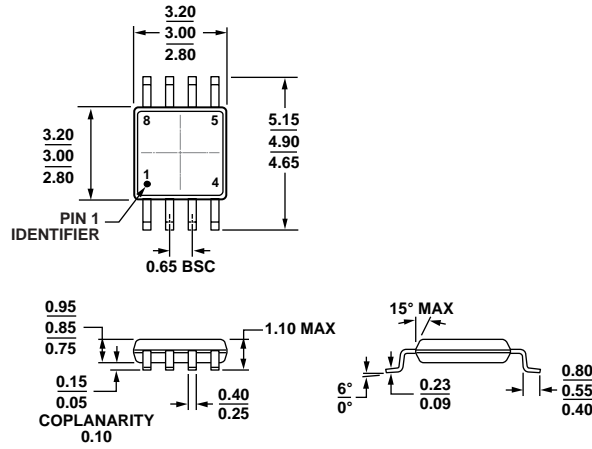
Figure 60. 5-Ball Wafer Level Chip Scale Package [WLCSP] (CB-5-1)
Dimensions shown in millimeters

02-15-2013-B



COMPLIANT TO JEDEC STANDARDS MO-178-AA
Figure 61. 5-Lead Small Outline Transistor Package [SOT-23] (RJ-5)
Dimensions shown in millimeters

11-01-2010-A

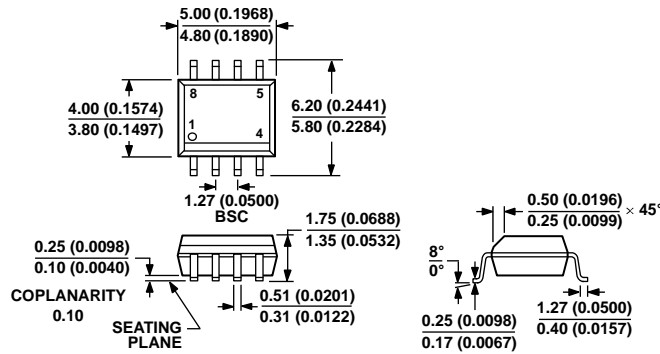


COMPLIANT TO JEDEC STANDARDS MO-187-AA

Figure 62. 8-Lead Mini Small Outline Package [MSOP] (RM-8)

Dimensions shown in millimeters

10-07-2008-B



COMPLIANT TO JEDEC STANDARDS MS-012-AA

CONTROLLING DIMENSIONS ARE IN MILLIMETERS; INCH DIMENSIONS (IN PARENTHESES) ARE ROUNDED-OFF MILLIMETER EQUIVALENTS FOR REFERENCE ONLY AND ARE NOT APPROPRIATE FOR USE IN DESIGN.

Figure 63. 8-Lead Standard Small Outline Package [SOIC_N] Narrow Body (R-8)

Dimensions shown in millimeters and (inches)

012407-A

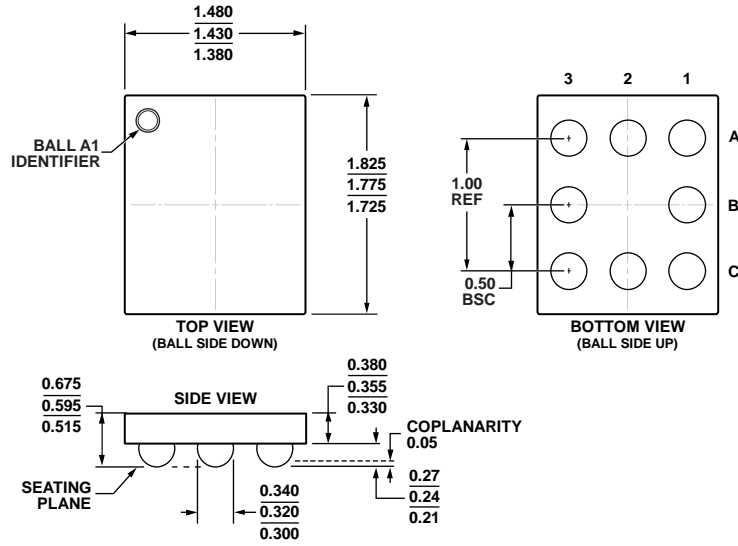
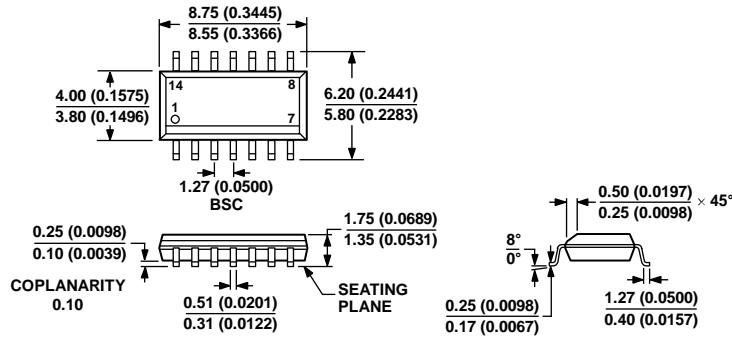


Figure 64. 8-Ball Wafer Level Chip Scale Package [WLCSPP]
(CB-8-1)
Dimensions shown in millimeters

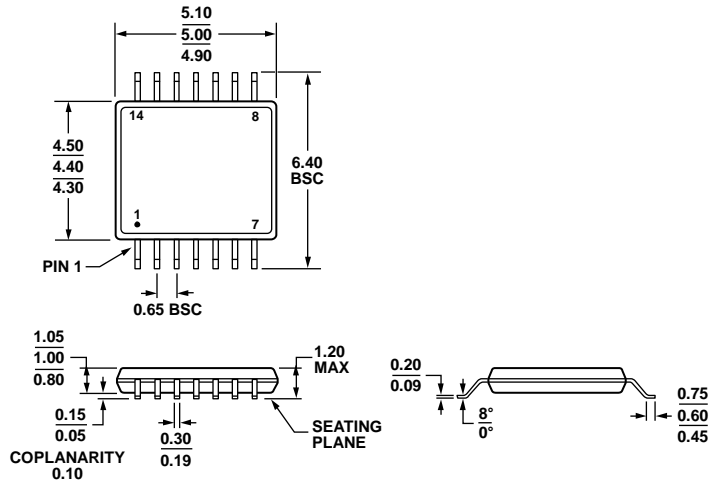
08-10-2012-A



COMPLIANT TO JEDEC STANDARDS MS-012-AB
CONTROLLING DIMENSIONS ARE IN MILLIMETERS; INCH DIMENSIONS
(IN PARENTHESES) ARE ROUNDED-OFF MILLIMETER EQUIVALENTS FOR
REFERENCE ONLY AND ARE NOT APPROPRIATE FOR USE IN DESIGN.

Figure 65. 14-Lead Standard Small Outline Package [SOIC_N]
Narrow Body (R-14)
Dimensions shown in millimeters and (inches)

060606-A



COMPLIANT TO JEDEC STANDARDS MO-153-AB-1

Figure 66. 14-Lead Thin Shrink Small Outline Package [TSSOP] (RU-14)

Dimensions shown in millimeters and (inches)

061908-A

ORDERING GUIDE

Model ¹	Temperature Range	Package Description	Package Option	Marking Code
AD8605ACBZ-REEL7	-40°C to +125°C	5-Ball WLCSP	CB-5-1	A1J
AD8605ARTZ-R2	-40°C to +125°C	5-Lead SOT-23	RJ-5	B3A#
AD8605ARTZ-REEL	-40°C to +125°C	5-Lead SOT-23	RJ-5	B3A#
AD8605ARTZ-REEL7	-40°C to +125°C	5-Lead SOT-23	RJ-5	B3A#
AD8606ARM-REEL	-40°C to +125°C	8-Lead MSOP	RM-8	B6A
AD8606ARMZ-R7	-40°C to +125°C	8-Lead MSOP	RM-8	B6A#
AD8606ARMZ-REEL	-40°C to +125°C	8-Lead MSOP	RM-8	B6A#
AD8606ARZ	-40°C to +125°C	8-Lead SOIC_N	R-8	
AD8606ARZ-REEL	-40°C to +125°C	8-Lead SOIC_N	R-8	
AD8606ARZ-REEL7	-40°C to +125°C	8-Lead SOIC_N	R-8	
AD8606ACBZ-REEL7	-40°C to +125°C	8-Ball WLCSP	CB-8-1	B6A#
AD8608ARZ	-40°C to +125°C	14-Lead SOIC_N	R-14	
AD8608ARZ-REEL	-40°C to +125°C	14-Lead SOIC_N	R-14	
AD8608ARZ-REEL7	-40°C to +125°C	14-Lead SOIC_N	R-14	
AD8608ARUZ	-40°C to +125°C	14-Lead TSSOP	RU-14	
AD8608ARUZ-REEL	-40°C to +125°C	14-Lead TSSOP	RU-14	

¹ Z = RoHS Compliant Part, # denotes RoHS compliant product (except for CB-5-1) may be top or bottom marked.

X-ON Electronics

Largest Supplier of Electrical and Electronic Components

Click to view similar products for [Precision Amplifiers](#) category:

Click to view products by [Analog Devices](#) manufacturer:

Other Similar products are found below :

[561681F](#) [LT6005HGN#PBF](#) [LT6238CGN#PBF](#) [LT6238HGN#PBF](#) [OP05CN8#PBF](#) [OP227GN#PBF](#) [LT6020IDD-1#PBF](#) [LT1124CS8#TR](#)
[NCV20166SN2T1G](#) [NCS21802MUTBG](#) [LT1637MPS8](#) [LT1498IS8](#) [LT1492CS8](#) [TLC27L7CP](#) [TLV2473CDR](#) [LMP2234AMA/NOPB](#)
[LMP7707MA/NOPB](#) [5962-8859301M2A](#) [LMP2231AMAE/NOPB](#) [LMP2234AMTE/NOPB](#) [LMC6022IM/NOPB](#) [LMC6024IM/NOPB](#)
[LMC6081IMX/NOPB](#) [LMP2011MA/NOPB](#) [LMP2231AMFE/NOPB](#) [LMP2232BMA/NOPB](#) [LMP2234AMAE/NOPB](#) [LMP7717MAE/NOPB](#)
[LMV2011MA/NOPB](#) [TLC2201AMDG4](#) [TLE2024BMDWG4](#) [TLV2474AQDRG4Q1](#) [TLV2472QDRQ1](#) [TLC4502IDR](#) [TLC27M2ACP](#)
[TLC2652Q-8DG4](#) [OPA2107APG4](#) [TL054AIDR](#) [TLC272CD](#) [AD8539ARMZ](#) [LTC6084HDD#PBF](#) [LT1638CMS8#TRPBF](#)
[LTC1050CN8#PBF](#) [LT1112ACN8#PBF](#) [LT1996AIDD#PBF](#) [LT1112CN8#PBF](#) [LTC6087CDD#PBF](#) [LT1078S8#PBF](#) [LT1079ACN#PBF](#)
[LTC6242HVCDHC#PBF](#)